FERMILAB-FN-0820-E

# Study of $b$-baryons at DØ in RunII of the Tevatron. $\Lambda_b$ *lifetime and* $\Xi_b^-$ *discovery.*

Eduard De La Cruz Burelo*
*University of Michigan*
(Dated: April 14, 2008)

The study of $b$-baryons is a unique opportunity at the Tevatron collider, which is the only running accelerator where these particles are expected to be produced. At the beginning of RunII of the Tevatron and after almost 30 years of the discovery of the $b$ quark at Fermilab, the lack of statistics had restricted our knowledge on $b$-baryons to the observation of the lightest $b$-baryon, the $\Lambda_b$, and to its lifetime measured in decays which did not allow a fully reconstruction of this particle. I present results of the search for $b$-baryons in the DØ experiment. As part of this program, a precise measurement of the $\Lambda_b$ lifetime was performed, and the discovery of the $\Xi_b^-$ resulted from an analysis of 1.3 fb$^{-1}$ of data collected with the D0 detector during 2002–2006.

## INTRODUCTION

The observation and measurement of properties of $B$ hadrons (particles which heavy constituent quark is a $b$ quark) has been an important part of the rich physics program of Tevatron experiments, CDF [1] and DØ [2]. Properties like the lifetime of $B$ hadrons provides information on the $b$ quark decay, and what is the role that play the lighter quarks which along with the $b$-quark form the $B$ hadron. Also, $b$-quark decays are related to the $V_{ub}$ and $V_{cb}$ elements of the CKM matrix, and B rare decays are always considered a playground to test extensions of the Standard Model of particles.

Since the discovery of the $b$ quark at Fermilab in 1977, and before RunII of Tevatron, all $b$-mesons in the ground state ($B^+(\bar{b}u)$, $B^0(\bar{b}d)$, $B_s(\bar{b}s$, and $B_c^+(\bar{b}c)$) have been experimentally established, but only the lightest $b$-baryon, the $\Lambda_b(bud)$, had been observed. During RunII of Tevatron a significant progress has been made in the $b$-baryon sector. The $\Lambda_b$ has been observed by both experiments, CDF and DØ, and its lifetime has been measured in different decays channels. Other $b$-baryons has been finally observed, and properties as their masses have been established with high precision [3–5].

In the first part of this note, a description of the $\Lambda_b$ observation and measurement of its lifetime in the DØ experiment, by reconstructing $\Lambda_b \to J/\psi\Lambda$ decays, is presented. An earlier difference between measurement and prediction created a great deal of interest on the $\Lambda_b$ lifetime, and it was named as the $\Lambda_b$ *lifetime puzzle*[6]. Recent theoretical calculations of $\tau(\Lambda_b)/\tau(B^0)$, which include next-to-leading order effects in QCD [7], corrections at $\mathcal{O}(1/m_b^4)$ in HQET [8], and lattice QCD studies [9], have led to a prediction of $\tau(\Lambda_b)/\tau(B^0) = 0.88\pm0.05$ [10], that significantly reduced this difference ( $\tau(\Lambda_b)/\tau(B^0) = 0.800 \pm 0.053$ was the world average in 2004 [11] ). However, a recent precise measurement [12] by CDF experiment reports a value of the $\Lambda_b$ lifetime consistent with $b$ meson lifetimes, and the ratio $\tau(\Lambda_b)/\tau(B^0)$ consistent with unity. This measurement, which statistically dominates the current world average, has turned around the $\Lambda_b$ lifetime puzzle, by making the prediction to be lower than the experimental measurement. DØ is currently the only other experiment that can measure this property of the $\Lambda_b$ to help settle this puzzle.

The second part of this note is dedicated to describe the discovery of the $\Xi_b^-(bsd)$, the first observed particle formed by a quark of each known family of matter. In the quark model the $\Xi_b^-$[24] is formed by the combination of a $b$, a $d$, and a $s$ quarks, and it is expected to have $J^P = 1/2^+$ although $I$, $J$ or $P$ have yet to be measured. Evidence for the $\Xi_b^-$ has been inferred from an excess of same sign $\Xi^\pm\ell^\pm$ events in jets which are interpreted as $\Xi_b^- \to \Xi^-\ell^-\bar{\nu}_\ell X$ [13]. From this decay mode, the average lifetime of the $\Xi_b^-$ is measured to be $1.42^{+0.28}_{-0.24}$ ps [14]. These semileptonic decays of the $\Xi_b^-$ did not allow for a mass measurement, but theoretical calculations of heavy quark effective theory [15] and nonrelativistic QCD [16] predict the $\Xi_b^-$ mass in the range $5.7 - 5.8$ GeV [17]. DØ experiment observed for first time the $\Xi_b^-$ baryon fully reconstructed in an exclusive decay, $\Xi_b^- \to J/\psi\,\Xi^-$, with $J/\psi \to \mu^+\mu^-$, $\Xi^- \to \Lambda\pi^-$, and $\Lambda \to p\pi^-$.

In spirit of being totally consistent with published results, most of the text describing data selection and fitting procedure in these two analyses has been taken from the $\Lambda_b$ lifetime [18] and $\Xi_b^-$ discovery [4] publications by the DØ experiment. However, explanations which were not included in the original publications (mainly due to lack of space) are added in many cases, and by having both analyses in single note, it would be clear how important for the $\Xi_b^-$ observation in DØ has been the study of the $\Lambda_b$ particle, on which almost all selection criteria for the $\Xi_b^-$ discovery is based.

* *E-mail address*: eduard@fnal.gov

## THE DØ DETECTOR

The D0 detector is described in detail elsewhere [2]. The components most relevant to these analyses are the central tracking system and the muon spectrometer. The central tracking system consists of a silicon microstrip tracker (SMT) and a central fiber tracker (CFT) that are surrounded by a 2 T superconducting solenoid. The SMT is optimized for tracking and vertexing for the pseudorapidity region $|\eta| < 3$ ($\eta = -\ln[\tan(\theta/2)]$ and $\theta$ is the polar angle) while the CFT has coverage for $|\eta| < 2$. Liquid-argon and uranium calorimeters in a central and two end-cap cryostats cover the pseudorapidity region $|\eta| < 4.2$. The muon spectrometer is located outside the calorimeter and covers the pseudorapidity region $|\eta| < 2$. It comprises a layer of drift tubes and scintillator trigger counters in front of 1.8 T iron toroids followed by two similar layers behind the toroids.

## $\Lambda_b$ LIFETIME MEASUREMENT

### Event selection

The search for $\Lambda_b \to J/\psi\Lambda$ decays begins with the reconstruction of $J/\psi$ candidates in the decay channel $J/\psi \to \mu^+\mu^-$, where the muon system of the DØ detector is used to confirm the muon candidates. Then these events containing a $J/\psi$ meson are searched for $\Lambda \to p\pi^-$ decays. $J/\psi$ and $\Lambda$ candidates are then combined to search for those decays coming from $\Lambda_b$ particles. Although specific triggers are not required for event selection, most of the selected events satisfy dimuon or muon triggers due to the present of a $J/\psi \to \mu^+\mu^-$ candidate in which muons are confirmed in the muon detector. However, to avoid a trigger bias in the lifetime measurement, events that depend on impact parameter based triggers are rejected. In addition, candidate events must have at least one primary vertex reconstructed.

To form a $J/\psi$ candidate, two oppositely charged tracks must originate from a common vertex with a $\chi^2$ probability greater than 1%, and have an invariant mass in the range of $2.8-3.35$ GeV , that approximately corresponds to $M_{J/\psi} \pm 3\sigma_{J/\psi}$, where $\sigma_{J/\psi}$ is the width of the $J/\psi$ signal observed in DØ and $M_{J/\psi}$ is the mass of the $J/\psi$ measured in DØ. Each track must either match hits in the muon system, or have calorimeter energies consistent with a minimum-ionizing particle. In addition, a minimum $p_T$ of 1.5 GeV and at least one CFT hit for each track is required, and at least one of the muons must have signatures in the three layers of the muon detector. Both tracks are required to have $p_T$ >2.5 GeV if they are in the region $|\eta|$ <1. The $J/\psi$ candidate is required to have a $p_T > 5$ GeV, and in addition, the distance between primary vertex and the dimuon vertex is required to be less than 10 cm.

The $\Lambda \to p\pi^-$ candidates are reconstructed from two oppositely charged tracks which must originate from a common vertex with a $\chi^2$ probability greater than 1%, and an invariant mass between $1.105 - 1.125$ GeV, that similar to the $J/\psi$ selection, approximately corresponds to three times the width of the observed $\Lambda$ signal around the mass of the $\Lambda$. The two tracks are collectively required to have no more than two hits in the tracking system before the vertex, and the track with the higher $p_T$ is assigned to be proton if positive and to be antiproton if negative. Monte Carlo studies show that this assignment gives nearly 100% correct combination. The $\Lambda$ is a particle that travels long distance in the detector before it decays, then tracks of its decay products must have a considerable impact parameter with respect to the primary vertex. To exploit this feature, the axial $\epsilon_T$ and stereo $\epsilon_L$ impact parameter projections of each track with respect to the primary vertex and their uncertainties are calculated, and the combined significance $(\epsilon_T/\sigma(\epsilon_T))^2 + (\epsilon_L/\sigma(\epsilon_L))^2$ is required to be greater than 9 for both tracks and greater than 16 for at least one of the tracks. To reduce combinatoric backgrounds, the $\Lambda$ decay distance from the primary vertex is required to be greater than 4 times its estimated uncertainty when this uncertainty is less than 0.5 cm.

The $\Lambda_b$ candidates are reconstructed by performing a constrained fit to a common vertex for the $\Lambda$ and the two tracks forming the $J/\psi$ candidate, with the latter constrained to the $J/\psi$ mass of 3.097 GeV/$c^2$ [19]. To suppress contamination from cascade decays of more massive baryons such as $\Sigma^0 \to \Lambda\gamma$ or $\Xi^0 \to \Lambda\pi^0$, the cosine of the angle between the $\boldsymbol{p}_T$ vector of the $\Lambda$ and the vector in the perpendicular plane from the $J/\psi$ vertex to the $\Lambda$ decay vertex is required to be larger than 0.9999. For $\Lambda$'s that decay from $\Lambda_b$ the cosine of this angle is very close to one. If more than one $J/\psi + \Lambda$ candidate is found in the event, the candidate with the best $\chi^2$ probability is selected as the $\Lambda_b$. The mass of $J/\psi + \Lambda$ combination is required to be within the range 5.1–6.1 GeV/$c^2$. For the choice of the final selection criteria, $S/\sqrt{S+B}$ is optimized, where $S$ and $B$ are the number of signal ($\Lambda_b$) and background candidates, respectively, by using Monte Carlo estimates for $S$ and data for $B$. As a result of this optimization, the $p_T$ of the $\Lambda$ is required to be greater than 2.4 GeV/$c$, and the total momentum for the $\Lambda_b$ is required to be greater than 5 GeV/$c$.

In order to test the selection and lifetime measurement procedure, simultaneously to the reconstruction of $\Lambda_b \to J\psi(\mu^+\mu^-)\Lambda(p\pi^-)$ decays, the well known $B^0$ meson is reconstructed in the topologically similar decay $B^0 \to J\psi(\mu^+\mu^-)K^0_S(\pi^+\pi^-)$, where a pion takes the place of the proton in the $\Lambda$ reconstruction to form a $K^0_S$. Same selection is applied for the $J/\psi$ reconstruction, and the $K^0_S \to \pi^+\pi^-$ selection follows the same criteria as for the $\Lambda$ reconstruction, except that for the $K^0_S$, the mass window is 0.460–0.525 GeV/$c^2$, and pion

mass assignments are used. In addition, the $p_T$ of the $K^0_S$ is required to be greater than 1.8 GeV/$c$ and $J/\psi + K^0_S$ candidates within 4.9–5.7 GeV/$c^2$ are considered for the $B^0$ search. Finally, any event which has been selected in the $\Lambda_b$ reconstruction is removed from the $B^0$ sample.

### Lifetime measuring technique

The decay time of a $\Lambda_b$ or $B^0$ is determined by measuring the distance traveled by the $b$ hadron candidate in a plane transverse to the beam direction, and then applying a correction for the Lorentz boost. The transverse decay length is defined as $L_{xy} = \boldsymbol{L}_{xy} \cdot \boldsymbol{p}_T / p_T$ where $\boldsymbol{L}_{xy}$ is the vector that points from the primary vertex to the $b$ hadron decay vertex and $\boldsymbol{p}_T$ is the transverse momentum vector of the $b$ hadron. The event-by-event value of the proper transverse decay length, $\lambda$, for the $b$ hadron candidate is given by:

$$\lambda = \frac{L_{xy}}{(\beta\gamma)^B_T} = L_{xy}\,\frac{cM_B}{p_T}, \qquad (1)$$

where $(\beta\gamma)^B_T$ and $M_B$ are the transverse boost and the mass of the $b$ hadron. In this measurement, the value of $M_B$ in Eq. 1 is set to the Particle Data Group (PDG) mass value of $\Lambda_b$ or $B^0$ [19]. In order to reduce background from mismeasurement of vertices, the uncertainty on $\lambda$ is required to be less than 500 $\mu$m.

A simultaneous unbinned maximum likelihood fit is performed to the mass and proper decay length distributions. The likelihood function $\mathcal{L}$ is defined by:

$$\begin{aligned}\mathcal{L} \;=\; & \tfrac{(n_s+n_b)^N}{N!}\exp\left(-n_s-n_b\right)\times \\ & \textstyle\prod_{j=1}^{N}\left[\frac{n_s}{n_s+n_b}\mathcal{F}^j_{\rm sig}+\frac{n_b}{n_s+n_b}\mathcal{F}^j_{\rm bkg}\right],\end{aligned} \qquad (2)$$

where $n_s$ and $n_b$ are the expected number of signal and background events in the sample, respectively. $N$ is the total number of events. $\mathcal{F}^j_{\rm sig}$ ($\mathcal{F}^j_{\rm bkg}$) is the product of three probability density functions that model the mass, proper decay length, and uncertainty on proper decay length distributions for the signal (background). The background is divided into two categories, prompt and non-prompt. The prompt background is primarily due to direct production of $J/\psi$'s which are then randomly combined with a $\Lambda$ or $K^0_S$ candidate in the event. The non-prompt background is mainly produced by the combination of $J/\psi$ mesons from $b$ hadron decays with $\Lambda$ or $K^0_S$ candidates present in the event.

For the signal, the mass distribution is modeled by a Gaussian function, and the $\lambda$ distribution is parametrized by an exponential decay convoluted with the resolution function:

$$G(\lambda_j,\sigma_j) = \frac{1}{\sqrt{2\pi}s\sigma_j}\exp\left[\frac{-\lambda_j^2}{2(s\sigma_j)^2}\right], \qquad (3)$$

where $\lambda_j$ and $\sigma_j$ represent $\lambda$ and its uncertainty, respectively, for a given decay $j$, and $s$ is a common scale parameter introduced in the fit to account for a possible mis-estimate of $\sigma_j$. The convolution is defined by:

$$S_\lambda(\lambda_j,\sigma_j) = \frac{1}{\lambda_B}\int_0^\infty G(x-\lambda_j,\sigma_j)\exp\left(\frac{-x}{\lambda_B}\right)dx, \qquad (4)$$

where $\lambda_B = c\tau_B$, and $\tau_B$ is the lifetime of the $\Lambda_b$ ($B^0$). The distribution of the uncertainty of $\lambda$ is modeled by an exponential function convoluted by a Gaussian.

For the background, the mass distribution of the prompt component is assumed to follow a flat distribution as observed in data when a cut of $\lambda$ >100 $\mu$m is applied. The non-prompt component is modeled with a second-order polynomial function. The $\lambda$ distribution is parametrized by the resolution function for the prompt component, and by the sum of negative and positive exponential functions for the non-prompt component. A positive and a negative exponential functions model combinatorial background, and an exponential function accounts for long-lived heavy flavor decays. The distribution of the uncertainty of $\lambda$ is modeled by two exponential functions convoluted by a Gaussian.

By minimizing $-2\ln\mathcal{L}$, it is found: $c\tau(\Lambda_b) = 365.1^{+39.1}_{-34.7}$ $\mu$m and $c\tau(B^0) = 450.0^{+23.5}_{-22.1}$ $\mu$m. From the fits, it is obtained $s = 1.41 \pm 0.05$ for the $\Lambda_b$ and $s = 1.41 \pm 0.03$ for the $B^0$. The numbers of signal decays are $171\pm20$ $\Lambda_b$ and $717\pm38$ $B^0$. Figures 1 and 2 show the mass and $\lambda$ distributions for the $\Lambda_b$ and $B^0$ candidates. Fit results are superimposed.

### Systematic uncertainties

Table I summarizes the systematic uncertainties considered in these lifetime measurements. The contribution from possible misalignment of the SMT detector was estimated in the first $\Lambda_b$ lifetime measurement to be 5.4 $\mu$m [20]. This was done by reconstructing the $B^0$ sample with a SMT geometry where the silicon sensors are moved from their nominal positions within the current alignment precision. Systematic uncertainties due to the modeling of the $\lambda$ and mass distributions are estimated by varying the parametrizations of the different components: (i) the resolution function is modeled by two Gaussian functions instead of one, (ii) the exponential functions in the non-prompt background are replaced by exponentials convoluted with the resolution function, (iii) a uniform background is added to account for outlier events (this has only a negligible effect), (iv) the positive and negative exponentials describing combinatorial non-prompt background are assumed to be symmetric, and (v) for the mass distribution of the non-prompt background, a linear function is used instead of the nominal quadratic form. To take into account correlations be-

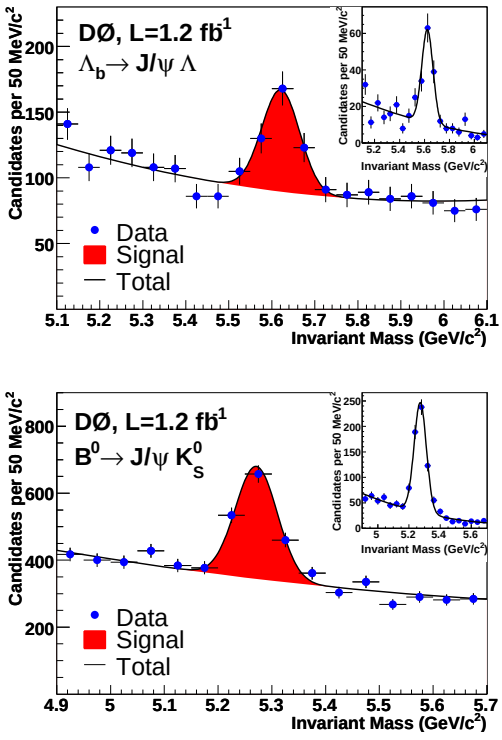


FIG. 1: Invariant mass distribution for $\Lambda_b$ (top) and $B^0$ (bottom) candidates with the fit results superimposed. The inserts show the mass distributions after requiring $\lambda/\sigma > 5$.

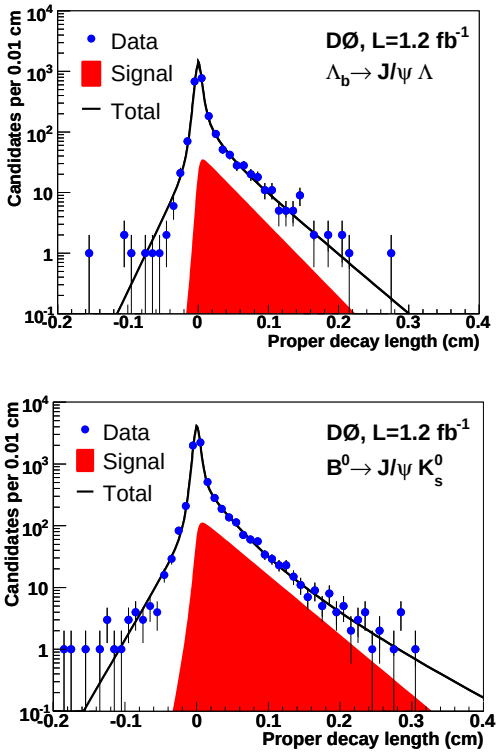


FIG. 2: Proper decay length distribution for $\Lambda_b$(top) and $B^0$(bottom) candidates, with the fit results superimposed. The shaded region represents the signal.

tween the effects of the different models, a fit that combines all different model changes is performed, and the difference between the result of this fit and the nominal fit is quoted as the systematic uncertainty.

The lifetime of the background events under the $\Lambda_b(B^0)$ signal is mostly modeled by events in the low and high mass sideband regions with respect to the peak. To estimate the effect of any difference between the lifetime distributions of these two regions, separate fits are performed to the $\Lambda_b$ ($B^0$) mass regions of 5.1–5.8 and 5.4–6.1 GeV/$c^2$ (4.9–5.45 and 5.1–5.7 GeV/$c^2$) where the contributions from high and low mass background events are reduced, respectively. The largest difference between these fits and the nominal fit is quoted as the systematic uncertainty due to this source.

Contamination of the $\Lambda_b$ sample by $B^0$ events that pass the $\Lambda_b$ selection is also considered. From Monte Carlo studies, it is estimated that 6.5% of $B^0$ events can pass the $\Lambda_b$ selection criteria. However, the invariant mass of $B^0$ events which contaminate the $\Lambda_b$ sample is distributed almost uniformly across the entire $\Lambda_b$ mass range, and their proper decay lengths therefore tend to be incorporated in the long-lived component of the background. In order to estimate any effect due to this possible contamination, any event which also passes the $B^0$ selection criteria is removed from the $\Lambda_b$ sample, and the lifetime fit is repeated to the remaining events. The difference between this and the nominal fit is quoted as a systematic uncertainty. For the $B^0$ lifetime, this source of systematic uncertainty is not considered since any event with a $\Lambda_b$ candidate is removed from the $B^0$ sample.

In addition to the systematic uncertainty studies, other several cross-checks on the lifetime measurements are performed. The $J/\psi$ vertex is used instead of the $b$ hadron vertex, the mass windows are varied, the reconstructed $b$ hadron mass is used instead of the PDG [19] value, and the sample is split into different pseudorapidity regions and different regions of azimuth. All results obtained with these variations are consistent with our measurement. The fitting procedure and selection criteria is also cross-checked by measuring the $\Lambda_b$ lifetime in Monte Carlo events. The lifetime obtained was consistent with the input value.

## Results

The results of the measurement of the $\Lambda_b$ and $B^0$ lifetimes are summarized as:

$$c\tau(\Lambda_b) = 365.1^{+39.1}_{-34.7}\ (\text{stat}) \pm 12.7\ (\text{syst})\ \mu\text{m}, \qquad (5)$$

TABLE I: Summary of systematic uncertainties in the measurement of $c\tau$ for $\Lambda_b$ and $B^0$ and their ratio. The total uncertainties are determined by combining individual uncertainties in quadrature.

| Source | $\Lambda_b$ ($\mu$m) | $B^0$ ($\mu$m) | Ratio |
|---|---|---|---|
| Alignment | 5.4 | 5.4 | 0.002 |
| Distribution models | 6.6 | 2.8 | 0.020 |
| Long-lived components | 6.0 | 13.6 | 0.022 |
| Contamination | 7.2 | – | 0.016 |
| Total | 12.7 | 14.9 | 0.034 |

$$c\tau(B^0) = 450.0^{+23.5}_{-22.1}\ (\text{stat}) \pm 14.9\ (\text{syst})\ \mu\text{m},$$

from which:

$$\tau(\Lambda_b) = 1.218^{+0.130}_{-0.115}\ (\text{stat}) \pm 0.042\ (\text{syst})\ \text{ps}, \quad (6)$$
$$\tau(B^0) = 1.501^{+0.078}_{-0.074}\ (\text{stat}) \pm 0.050\ (\text{syst})\ \text{ps}.$$

These can be combined to determine the ratio of lifetimes:

$$\frac{\tau(\Lambda_b)}{\tau(B^0)} = 0.811^{+0.096}_{-0.087}\ (\text{stat}) \pm 0.034\ (\text{syst}), \quad (7)$$

The systematic uncertainty on the ratio is computed by calculating the ratio for each systematic source and quoting the deviation in the ratio as the systematic uncertainty due to that source. All systematics are combined in quadrature as shown in Table I. The main contribution to the systematic uncertainty of the lifetime ratio is due to the long-lived component of the $B^0$ sample. This is expected since the $B^0$ is more likely than the $\Lambda_b$ to be contaminated by mis-reconstructed $b$ mesons due to its lower mass.

The measurement is consistent with the world average [19], and the ratio of $\Lambda_b$ to $B^0$ lifetimes is consistent with the most recent theoretical predictions [10].

## $\Xi_b^-$ DISCOVERY

The decay $\Xi_b^- \to J/\psi\Xi^-$ has topological characteristics which help to reduce combinatorial background, but these characteristics also considerably reduce the reconstruction efficiency for this particle. Figure 3 shows a drawing of this decay. This decay includes the reconstruction of three particles: the $J/\psi \to \mu^+\mu^-$, $\Lambda \to p\pi^-$, and $\Xi^- \to \Lambda\pi^-$. The $\Lambda$ and $\Xi^-$ have a lifetime of the order of centimeters, while the $\Xi_b^-$ should have a lifetime of the order of microns. The $\Xi_b^-$ has a decay vertex displaced from the primary vertex and its decay product includes a particle, the $\Xi^-$, which travels a long distance in the detector before it decays to a pion and another very long-lived particle, the $\Lambda$. Three charged particles in the final state, $(p, \pi^-, \pi^-)$ should have a significant impact parameter with respect to the primary vertex. This

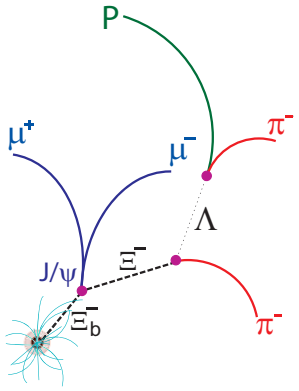


FIG. 3: Decay $\Xi_b^- \to J/\psi\Xi^-$.

final characteristics is what considerably reduces the reconstruction efficiency of the $\Xi_b^- \to J/\psi\Xi^-$ decay. This led to a reprocessing of dimuon events with an extended version of the tracking algorithm to allow the reconstruction of tracks with very high impact parameters and low $p_T$.

### Event selection

The $\Xi_b^-$ reconstruction starts by searching for events with $J/\psi$ mesons. Then these events are searched for $\Lambda$ candidates. These $\Lambda$ candidates are combined with an extra charged track in the event to reconstruct $\Xi^- \to \Lambda\pi^-$ decays. Then $J/\psi$ and $\Xi^-$ candidates are combined to reconstruct the $\Xi_b^- \to J/\psi\Xi^-$ decays.

The reconstruction of $J/\psi \to \mu^+\mu^-$ and $\Lambda \to p\pi^-$ decays follows the same selection as for the $\Lambda_b$ lifetime measurement. However, events containing a $J/\psi$ candidate were reprocessed with a version of the track reconstruction algorithm that improves the efficiency for tracks with low $p_T$ and high impact parameters. Consequently, the efficiencies for $K^0_S$, $\Lambda$, and $\Xi^-$ reconstruction are significantly increased. Figure 4(a) shows for comparison, the $\Xi^-$ reconstruction (as described below) before and after reprocessing events with at least a $J/\psi$ candidate.

The reconstruction of $\Xi^- \to \Lambda\pi^-$ decays is inspired on the selection criteria applied to $\Lambda \to p\pi^-$ decays, which is as the $\Xi^-$, a particle that travels long distance in the detector before it decays, and in addition the $\Lambda$ has been studied in the $\Lambda_b \to J/\psi\Lambda$ reconstruction. The $\Xi^-$ candidates are reconstructed by combining $\Lambda$ candidates with negatively charged tracks (excluding from the list of tracks the proton and pion tracks from $\Lambda$ decays) with a pion mass assigned. The $\Lambda$ and the $\pi^-$ must originate from a common vertex with a $\chi^2$ probability greater than 1%. The $\Lambda$ decay distance in the transverse plane (the plane perpendicular to the beam direction) measured with respect to the $\Xi^-$ vertex is re-

quired to have a uncertainty less than 0.5 cm. The combined significance $(\epsilon_T/\sigma(\epsilon_T))^2 + (\epsilon_L/\sigma(\epsilon_L))^2$ of the $\pi^-$ is required to be greater than 9. To reduce combinatoric backgrounds, the $\Xi^-$ decay distance from the primary vertex is required to be greater than 4 times its estimated uncertainty when this uncertainty is less than 0.5 cm. In addition, the decay distance in the transverse plane measured with respect to the $J/\psi$ vertex is required to have a uncertainty less than 0.5 cm.

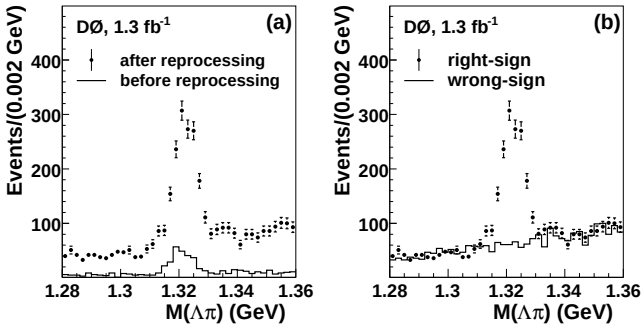


FIG. 4: Invariant mass distributions of the $\Lambda\pi$ pair before the $\Xi_b^-$ reconstruction for (a) the right-sign $\Lambda\pi^-$ combinations before and after reprocessing and (b) the right-sign $\Lambda\pi^-$ and the wrong-sign $\Lambda\pi^+$ combinations after reprocessing. The reprocessing significantly increases the $\Xi^-$ yield. Fits to the post-reprocessing distributions of the right-sign combination with a Gaussian signal and a first-order polynomial background yield $603 \pm 34$ $\Xi^-$'s and $548 \pm 31$ $\overline{\Xi}^+$'s.

The two pions from $\Xi^- \to \Lambda\pi^- \to (p\pi^-)\pi^-$ decays (right-sign) have the same charge. Consequently, the combination $\Lambda\pi^+$ (wrong-sign) events form an ideal control sample for background studies. Figure 4(b) compares mass distributions of the right-sign $\Lambda\pi^-$ and the wrong-sign $\Lambda\pi^+$ combinations. The $\Xi^-$ mass peak is evident in the distribution of the right-sign events. A $\Lambda\pi^-$ pair is considered to be a $\Xi^-$ candidate if its mass is within the range $1.305 < M(\Lambda\pi^-) < 1.340$ GeV.

To reconstruct $\Xi_b^- \to J/\psi\Xi^-$ decays, $J/\psi$ and $\Xi^-$ candidates are required to be in the same semi-hemisphere in the transverse plane and must have a common vertex with a $\chi^2$ <20. Backgrounds from mismeasurements are reduced by requiring uncertainties of the proper decay length of the $J/\psi\,\Xi^-$ vertex to be less than 0.05 cm in the transverse plane. A total of 2308 events remains after this preselection. The wrong-sign events are subjected to the same preselection as the right-sign events. A total of 1124 wrong-sign events is selected as the control sample.

Several distinctive features of the $\Xi_b^- \to J/\psi\,\Xi^- \to J/\psi\,\Lambda\pi^- \to (\mu^+\mu^-)\,(p\pi^-)\pi^-$ decay are utilized to further suppress backgrounds. The wrong-sign background events $(\Lambda\pi^+)$, $\Lambda$ and $J/\psi$ signals from $\Lambda_b \to J/\psi(\mu^+\mu^-)\Lambda(p\pi^-)$ decays from data, and Monte Carlo signal $\Xi_b^-$ events are used for studying additional event selection criteria. Protons and pions from the $\Xi^-$ decays of the $\Xi_b^-$ events are expected to have higher momenta than those from most of the background processes. Therefore, protons are required to have $p_T > 0.7$ GeV. Similarly, minimum $p_T$ requirements of 0.3 and 0.2 GeV are imposed on pions from $\Lambda$ and $\Xi^-$ decays, respectively. These requirements remove 91.6% of the wrong-sign background events while keeping 68.7% of the Monte Carlo $\Xi_b^-$ signal events. Figure 5 shows a simultaneous unbinned log-likelihood fit to the invariant mass and $p_T(\pi^-)$ distributions from $\Lambda_b \to J/\psi(\mu^+\mu^-)\Lambda(p\pi^-)$ decays in data, from where the $p_T > 0.3$ GeV cut for the pion from $\Lambda \to p\pi^-$ decays is selected. The $p_T(\pi^-)$ distribution for signal presents a long tail and the selected cut is near the maximum of the $p_T(\pi^-)$ distribution. Similarly, Fig. 6 shows the comparison of the $p_T(\pi^-)$ distributions from wrong-sign $(\Lambda\pi^+)$ background and $\Xi_b^-$ Monte Carlo events. The selected $p_T(\pi^-) > 0.2$ GeV cut removes a large amount of background while keeping most of the signal events.

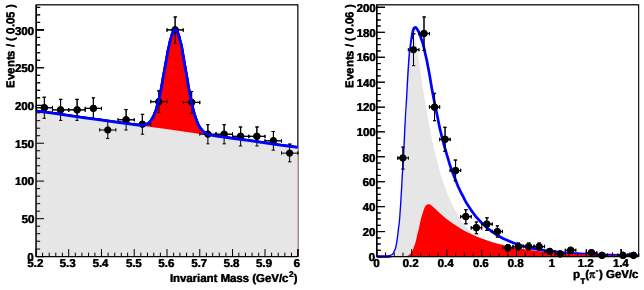


FIG. 5: Transverse momentum distribution of $\pi^-$ from the reconstructed decays $\Lambda_b \to J/\psi(\mu^+\mu^-)\Lambda(p\pi^-)$ in data. In the right is presented the mass distribution of the $\Lambda_b$ candidates, and in the left the $p_T(\pi^-)$ distribution with a fit superimposed. Red-filled region represents the signal and gray-filled region the background.

Backgrounds from combinatorics and other $b$ hadrons are reduced by using topological decay information. Contamination from decays such as $B^- \to J/\psi\,K^{*-} \to J/\psi\,K_S^0\pi^-$ and $B^0 \to J/\psi\,K^{*-}\pi^+ \to J/\psi\,(K_S^0\pi^-)\pi^+$, where all tracks in the combination $\mu^+\mu^-\Lambda\pi^-$ originate from the same vertex, are suppressed by requiring the $\Xi^-$ candidates to have decay lengths greater than 0.5 cm and $\cos(\theta) > 0.99$, as the $\Xi^-$ baryons in Monte Carlo have an average decay length of 4.8 cm. Here $\theta$ is the angle between the $\Xi^-$ direction and the direction from the $\Xi^-$ production vertex to its decay vertex in the transverse plane. Figure 7 shows the comparison of $\cos(\theta)$ distributions from wrong-sign background and $\Xi_b^-$ Monte Carlo events. From this comparison the cut $\cos(\theta) > 0.99$ is selected. These two requirements on the $\Xi^-$ reduce the background by an additional 56.4%, while removing only 1.7% of the Monte Carlo signal events.

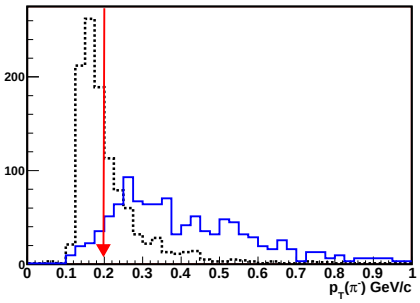


FIG. 6: Comparison of the pion (from $\Xi^-$ decays) $p_T$ distribution in wrong-sign background events and Monte Carlo signal events. Solid line in blue represents the signal and the dashed black line the background. Signal has been scaled to the same number of background events. The red arrow shows the selected $p_T$ cut.

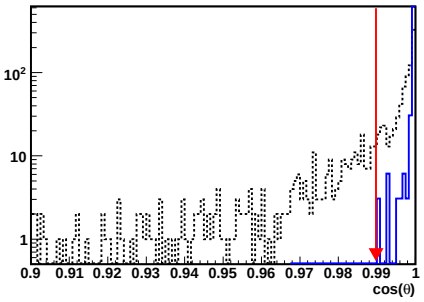


FIG. 7: Comparison of the $\Xi^-$ collinearity distribution in wrong-sign background events and Monte Carlo signal events, after pre-selection cuts. Solid line in blue represents the signal and the dashed black line the background. Signal has been scaled to the same number of background events. The red arrow shows the selected cut.

Finally, $\Xi_b^-$ baryons are expected to have a sizable lifetime. To reduce prompt backgrounds, the transverse proper decay length significance of the $\Xi_b^-$ candidates is required to be greater than two. This final criterion retains 83.1% of the Monte Carlo signal events but only 43.9% of the remaining background events.

In the data, 51 events with the $\Xi_b^-$ candidate mass between 5.2 and 7.0 GeV pass all selection criteria. Figure 8 shows the $\Xi_b^-$ candidates in the remaining events. An excess of events is observed near to 5.8 GeV. The mass range 5.2–7.0 GeV is chosen to be wide enough to encompass masses of all known $b$ hadrons as well as the predicted mass of the $\Xi_b^-$ baryon. The candidate mass, $M(\Xi_b^-)$, is calculated as $M(\Xi_b^-) = M(J/\psi\,\Xi^-) - M(\mu^+\mu^-) - M(\Lambda\pi^-) + M_{\rm PDG}(J/\psi) + M_{\rm PDG}(\Xi^-)$ to improve the resolution. Here $M(J/\psi\,\Xi^-)$, $M(\mu^+\mu^-)$, and $M(\Lambda\pi^-)$ are the reconstructed masses while $M_{\rm PDG}(J/\psi)$ and $M_{\rm PDG}(\Xi^-)$ are taken from Ref. [19]. A number of

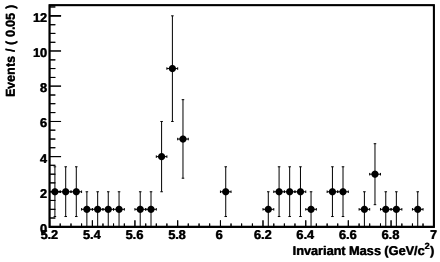


FIG. 8: $\Xi_b^-$ mass distribution from data after all selection cuts have been applied.

cross checks are performed to ensure the observed peak is not due to artifacts of the analysis: (1) The $J/\psi\,\Lambda\pi^+$ mass distribution of the wrong-sign events, shown in Fig. 9(top), is consistent with a flat background. (2) The event selection is applied to the sideband events of the $\Xi^-$ mass peak, requiring $1.28 < M(\Lambda\pi^-) < 1.36$ GeV but excluding the $\Xi^-$ mass window. Similarly, the selection is applied to the $J/\psi$ sideband events with $2.5 < M(\mu^+\mu^-) < 2.7$ GeV. The high-mass sideband is not considered due to potential contamination from $\psi'$ events. As shown in Fig. 9(middle and bottom), no evidence of a mass peak is present for either $(\mu^+\mu^-)\,(p\pi^-)\pi^-$ distribution. (3) Though most backgrounds from other $b$ hadron production are removed by the $\Xi^-$ reconstruction and its selection, the possibility of a fake signal due to the residual $b$ hadron background is investigated by applying the final $\Xi_b^-$ selection to high statistics Monte Carlo samples of $B^- \to J/\psi\,K^{*-} \to J/\psi\,K_S^0\pi^-$, $B^0 \to J/\psi\,K_S^0$, and $\Lambda_b \to J/\psi\,\Lambda$. No indication of a mass peak is observed in the reconstructed $J/\psi\,\Xi^-$ mass distributions. (4) The mass distributions of $J/\psi$, $\Xi^-$, and $\Lambda$ are investigated by relaxing the mass requirements on these particles one at a time for events both in the $\Xi_b^-$ signal region and the sidebands. The numbers of these particles determined by fitting their respective mass distribution are fully consistent with the quoted numbers of signal events plus background contributions. (5) The robustness of the observed mass peak is tested by varying selection criteria within reasonable ranges. All studies confirm the existence of the peak at the same mass.

### $\Xi_b^-$ mass measurement and signal significance

Interpreting the peak as $\Xi_b^-$ production, candidate masses are fitted with the hypothesis of a signal plus background model using an unbinned likelihood method. The signal and background shapes are assumed to be Gaussian and flat, respectively. The fit results in a $\Xi_b^-$ mass of $5.774 \pm 0.011$ GeV with a width of $0.037 \pm 0.008$ GeV and a yield of $15.2 \pm 4.4$ events. Where all

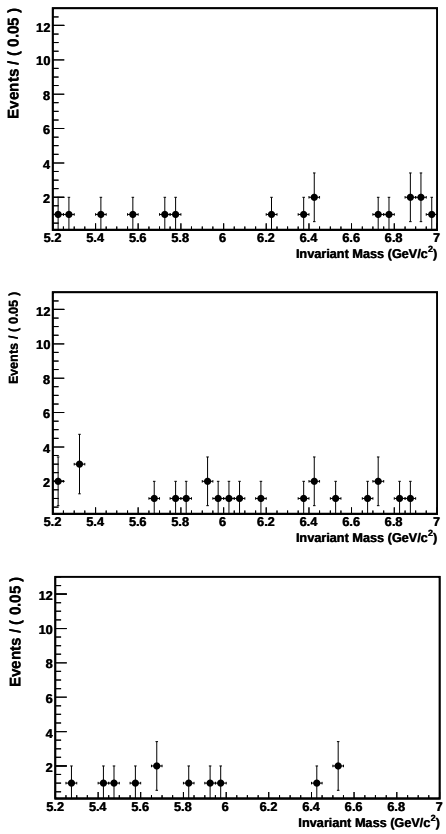


FIG. 9: Invariant mass distribution of background events from wrong-sign combinations (top), $\Xi^-$ sideband events (middle), and $J/\psi$ sideband events (bottom).

uncertainties are statistical. Following the same procedure, a fit to the Monte Carlo $\Xi_b^-$ events yields a mass of $5.839 \pm 0.003$ GeV, in good agreement with the 5.840 GeV input mass. The fitted width of the Monte Carlo mass distribution is $0.035 \pm 0.002$ GeV, consistent with the 0.037 GeV obtained from the data. Since the intrinsic decay width of the $\Xi_b^-$ baryon in the Monte Carlo is negligible, the width of the mass distribution is thus dominated by the detector resolution.

To assess the significance of the signal, the likelihood, $\mathcal{L}_{s+b}$, of the signal plus background fit above is first determined. The fit is then repeated using the background-only model, and a new likelihood $\mathcal{L}_b$ is found. The logarithmic likelihood ratio $\sqrt{2\ln(\mathcal{L}_{s+b}/\mathcal{L}_b)}$ indicates a statistical significance of $5.5\sigma$, corresponding to a probability of $3.3 \times 10^{-8}$ from background fluctuation for observing a signal that is equal to or more significant than what is seen in the data. Including systematic effects from the mass range, signal and background models, and the track momentum scale results in a minimum significance of $5.3\sigma$ and a $\Xi_b^-$ yield of $15.2 \pm 4.4\,(\text{stat.})^{+1.9}_{-0.4}\,(\text{syst.})$. The significance can also be estimated from the numbers of candidate events and estimated background events. In

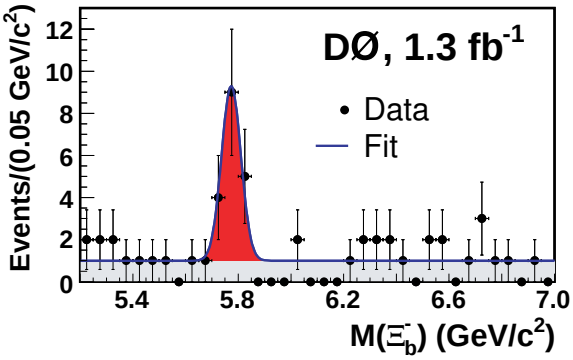


FIG. 10: Decay $\Xi_b^- \to J/\psi\Xi^-$.

the mass region of 2.5 times the fitted width centered on the fitted mass, 19 candidate events (8 $J/\psi\,\Xi^-$ and 11 $J/\psi\,\overline{\Xi}^+$) are observed while $14.8 \pm 4.3\,(\text{stat.})^{+1.9}_{-0.4}\,(\text{syst.})$ signal and $3.6 \pm 0.6\,(\text{stat.})^{+0.4}_{-1.9}\,(\text{syst.})$ background events are estimated from the fit. The probability of backgrounds fluctuating to 19 or more events is $2.2 \times 10^{-7}$, equivalent to a Gaussian significance of $5.2\sigma$.

Potential systematic biases on the measured $\Xi_b^-$ mass are studied for the event selection, signal and background models, and the track momentum scale. Varying cut values and using a multivariate technique of different variables for event selection leads to a maximum change of 0.020 GeV in the $\Xi_b^-$ mass. Subtracting an estimated statistical contribution to the change, a conservative $\pm 0.015$ GeV systematic uncertainty is assigned due to the event selection. Using double Gaussians for the signal model, a first-order polynomial for the background model, or fixing the mass resolution to that obtained from the Monte Carlo $\Xi_b^-$ events all lead to negligible changes in the mass. The mass, calculated using the world average values [19] of intermediate particle masses above, is found to have a weak dependence on the track momentum scale. This has been verified using the $\Lambda_b \to J/\psi\,\Lambda$ and $B^0 \to J/\psi\,K_S^0$ events observed in the data. A systematic uncertainty of $\pm 0.002$ GeV is assigned, corresponding to the mass difference between our measurement and the world average [19] for the $\Lambda_b$ and $B^0$ hadrons. Adding in quadrature, a total systematic uncertainty of $\pm 0.015$ GeV is obtained to yield the measured $\Xi_b^-$ mass: $5.774 \pm 0.011\,(\text{stat.}) \pm 0.015\,(\text{syst.})$ GeV.

### Relative production ratio

In addition to the observation and mass measurement of the $\Xi_b^-$ baryon, its $\sigma \times \mathcal{B}$ relative to that of the $\Lambda_b$

baryon is calculated using

$$\frac{\sigma(\Xi_b^-) \times \mathcal{B}(\Xi_b^- \to J/\psi\,\Xi^-)}{\sigma(\Lambda_b) \times \mathcal{B}(\Lambda_b \to J/\psi\,\Lambda)} = \frac{\epsilon(\Lambda_b \to J/\psi\,\Lambda)}{\epsilon(\Xi_b^- \to J/\psi\,\Xi^-)} \frac{N_{\Xi_b^-}}{N_{\Lambda_b}}$$

where $N_{\Xi_b^-}$ and $N_{\Lambda_b}$ are the numbers of $\Xi_b^-$ and $\Lambda_b$ events reconstructed in data. Analyzing the same data (reprocessed data in difference with that used for the $\Lambda_b$ lifetime measurement) and using the similar event selection criteria and fitting procedure as the $\Xi_b^-$ analysis, a yield of $240 \pm 30\,(\text{stat.}) \pm 12\,(\text{syst.})$ $\Lambda_b$ baryons is determined. The efficiencies to reconstruct the decays, $\epsilon(\Xi_b^-)$ and $\epsilon(\Lambda_b)$, are determined by Monte Carlo simulation, and the efficiency ratio, $\epsilon(\Lambda_b)/\epsilon(\Xi_b^-)$, is found to be $4.4 \pm 1.3$. The uncertainty on $\epsilon(\Lambda_b)/\epsilon(\Xi_b^-)$ arises from Monte Carlo modeling (27%), Monte Carlo statistics (10%), the reconstruction of the additional pion in the $\Xi_b^-$ decay (7%), and the $\Xi_b^-$ mass difference between data and Monte Carlo (5%). The largest component, Monte Carlo modeling uncertainty, is due to the difference in the efficiency ratio with and without Monte Carlo reweighting. This reweighting is needed to match Monte Carlo and data momentum distributions. The efficiency ratio is found to be insensitive to changes in $\Lambda_b$ and $\Xi_b^-$ production models. Many other systematic uncertainties on the efficiencies themselves tend to cancel in the ratio of the efficiencies. The relative production ratio is found to be $0.28 \pm 0.09\,(\text{stat.})^{+0.09}_{-0.08}\,(\text{syst.})$.

## SUMMARY

The $\Lambda_b$ lifetime measurement by the DØ experiment presented here is consistent with a $\Lambda_b$ lifetime shorter than the lifetime of $b$ mesons. In addition, DØ also measured the $\Lambda_b$ lifetime in semileptonic decays [21]. This independent measurement is consistent with the lifetime measured in the exclusive $\Lambda_b \to J/\psi\Lambda$ decay channel. When both DØ measurements are combined, it is found $\tau(\Lambda_b) = 1.251^{+0.102}_{-0.096}$ ps, what is less consistent with the CDF measurement $\tau(\Lambda_b) = 1.593^{+0.089}_{-0.085}$ ps. However, within the current precision it is not possible to settle the question of the lifetime puzzle, at least not from the experimental side. More statistics is needed for this.

Before RunII of the Tevatron, the experimental situation of $b$ baryons was not yet quite conclusive, with only the $\Lambda_b$ experimentally established. However, the observation of new heavy baryon states at Tevatron experiments has been prolific in Run II. In addition to the $\Xi_b^-$ baryon observed by DØ and also reported by CDF [5], other states, $\Sigma_b^{\pm}$ and $\Sigma_b^{*\pm}$, have been also observed [3]. These observations have allowed to compare experimental measurements with QCD potential models and lattice QCD predictions for mass of heavy baryons. Prediction and experiment agree very well, proving once more the success of the quark model. With more statistics, other properties besides masses could be measured, and search of physics beyond the Standard Model in $b$ baryons [22, 23] would be possible.


[1] CDF Collaboration, F. Abe *et al.*, Nucl. Instrum. Methods Phys. Res. A **271**, 388 (1998);
[2] V.M. Abazov *et al.* (D0 Collaboration), Nucl. Instrum. Methods A **565**, 463 (2006).
[3] A. Abulencia *et al.*, Phys. Rev. Lett. **99**, 202001 (2007).
[4] V.M. Abazov *et al.* (D0 Collaboration), Phys. Rev. Lett. **99**, 052001 (2007).
[5] A. Abulencia *et al.*, Phys. Rev. Lett. **99**, 052002 (2007).
[6] F. Gabbiani *et al.* Phys. Rev. Lett. **D** 68, (2003) 114006-1-4.
[7] E. Franco *et al.*, Nucl. Phys. B **633**, 212 (2002).
[8] F. Gabbiani, A. I. Onishchenko, A. A. Petrov, Phys. Rev. D **68**, 114006 (2003).
[9] M. Di Pierro *et al.*, Phys. Lett. B **468**, 143 (1999).
[10] C. Tarantino, Nucl. Phys. B **156**, (Proc. Suppl.), 33 (2006).
[11] S. Eidelman et al. (PDG 2004), Phys. Lett. B **592**, 1 (2004).
[12] A. Abulencia *et al.*, Phys. Rev. Lett. **98**, 122001 (2007).
[13] J. Abdallah *et al.* (DELPHI Collaboration), Eur. Phys. J. **C44**, 299 (2005); D. Buskulic *et al.* (ALEPH Collaboration), Phys. Lett. B **384**, 449 (1996).
[14] E. Barberio *et al.* (Heavy Flavor Averaging Group Collaboration), `arXiv:0704.3575`.
[15] N. Isgur and M.B. Wise, Phys. Rev. Lett. **66**, 1130 (1991).
[16] G.T. Bodwin, E. Braaten, G.P. Lepage, Phys. Rev. D **51**, 1125 (1995); erratum-*ibid*, Phys. Rev. D **55** 5853 (1997).
[17] E. Jenkins, Phys. Rev. D **55**, R10 (1997); *ibid*, Phys. Rev. D **54**, 4515 (1996); N. Mathur, R. Lewis and R.M. Woloshyn, Phys. Rev. D **66**, 014502 (2002).
[18] V.M. Abazov *et al.* (D0 Collaboration), Phys. Rev. Lett. **99**, 142001 (2007).
[19] W. M. Yao *et al.*, J. Phys. G **33**, 1 (2006).
[20] V. Abazov *et al.*, Phys. Rev. Lett. **94**, 102001 (2005).
[21] V.M. Abazov *et al.* (D0 Collaboration), Phys. Rev. Lett. **99**, 182001 (2007).
[22] I. Dunietz, z. Phys. C **56**, 129 (1992).
[23] C.Q. Gen *et al.*, Phys. Rev. D **65**, 0191502 (2002).
[24] Charge conjugation is always assumed for this state